Published in final edited form as:
J Neurochem. 2010 April ; 113(2): 374–388. doi:10.1111/j.1471-4159.2010.06592.x.

A Novel, High-Efficiency Cellular Model of Fibrillar α-Synuclein Inclusions and the Examination of Mutations that Inhibit Amyloid Formation

Elisa A. Waxman and **Benoit I. Giasson**
Department of Pharmacology, University of Pennsylvania, Philadelphia, PA

Abstract

Intracytoplasmic alpha-synuclein (α-syn) amyloidogenic inclusions are a major pathological feature of Parkinson's disease, dementia with Lewy body disease, and multiple systems atrophy. The mechanisms involved in the formation and inhibition of these aggregates are areas of intense investigation. The present study characterizes a novel cellular model for the study of α-syn aggregation, incorporating nucleation-dependent aggregation and a new function for calcium phosphate precipitation. Cultured cells were readily induced to develop large, cytoplasmic α-syn filamentous aggregates that were hyperphosphorylated, often ubiquitinated and thioflavin positive. These cellular aggregates formed in the majority of transfected cells and recruited approximately half of endogenously expressed α-syn. Using this system, we examined single-point mutations that inhibit α-syn amyloid formation *in vitro*. Three mutations (V66P, T72P, and T75P) significantly hindered α-syn aggregation in this cell model. The T75P mutant, which could abrogate amyloid formation of wild-type α-syn *in vitro*, did not prevent wild-type α-syn cellular aggregates. These studies suggest that the propensity of α-syn to form cellular aggregates may be more pronounced than in isolated *in vitro* studies. This novel high-efficiency cellular model of α-syn aggregation is a valuable system that may be used to further understand α-syn aggregation and allow for the generation of future therapeutics.

Keywords

α-synuclein; Parkinson's disease; phosphorylation; fibrillization; cellular model; inhibitors; nucleation

Parkinson's disease (PD) is the most common movement neurodegenerative disorder and is characterized by a loss of dopaminergic neurons in the substantia nigra pars compacta. Pathological analysis of PD brains reveals intracytoplasmic, perikaryal inclusions, known as Lewy bodies (LBs) in some of the remaining dopaminergic neurons, as well as similar inclusions in neuronal processes, termed Lewy neurites (LNs) (Goedert 2001;von Bohlen Und 2004;Lee and Trojanowski 2006). The major component of LBs and LNs is α-synuclein (α-syn), a 140 amino acid protein that is normally soluble and localized to neuronal synaptic terminals (Goedert 2001;von Bohlen Und 2004;Lee and Trojanowski 2006;Sidhu *et al.* 2004). A role for α-syn in the pathophysiology of PD is further supported by several missense mutations in α-syn and short chromosomal duplications and triplications that include the α-syn gene, which have been identified in familial forms of PD (Forman *et al.* 2005;Polymeropoulos *et al.* 1997). Furthermore, α-syn is the major component of

Address correspondence to: Dr. Benoit I. Giasson, Department of Pharmacology, University of Pennsylvania School of Medicine, 3620 Hamilton Walk, 125 John Morgan Building, Philadelphia, PA 19104-6084; Tel: 215-573-6012; Fax: 215-573-2236; giassonb@mail.med.upenn.edu..

pathological inclusions in other neurodegenerative diseases, including dementia with Lewy bodies (DLB), Lewy body variant of Alzheimer's disease (LBVAD), and multiple systems atrophy (MSA), which are collectively termed α-synucleinopathies (Duda *et al.* 2000;Lippa *et al.* 1999;Spillantini *et al.* 1997;Spillantini *et al.* 1998;Tu *et al.* 1998;Goedert 2001;Forman *et al.* 2005).

α-Syn aberrantly polymerizes into 10–15 nm amyloidogenic fibrils that associate to form cellular inclusions, which can contribute to the pathogenesis of PD (Goedert 2001;von Bohlen Und 2004;Lee and Trojanowski 2006). These inclusions can be detected with amyloid binding dyes, such as thioflavin and Congo Red or derivatives (Crystal *et al.* 2003;Conway *et al.* 2000). Aggregated α-syn in these inclusions also has several modifications, including ubiquitination (Sampathu *et al.* 2003) and hyperphosphorylation (Fujiwara *et al.* 2002;Kahle *et al.* 2002;Anderson *et al.* 2006;Nishie *et al.* 2004;Neumann *et al.* 2002;Waxman and Giasson 2008).

Recombinant α-syn can readily polymerize *in vitro* into amyloidogenic fibrils, which are structurally similar to pathological inclusions (Conway *et al.* 1998;Giasson *et al.* 1999;Hashimoto *et al.* 1998;Giasson *et al.* 2001). The middle hydrophobic region of α-syn plays a critical role in amyloid formation (Giasson *et al.* 2001;Waxman *et al.* 2009b;Zibaee *et al.* 2007), such that deletion of several hydrophobic stretches or single-point mutations in this region can prevent polymerization into mature amyloid (Biere *et al.* 2000;Du *et al.* 2003;Zibaee *et al.* 2007;Giasson *et al.* 2001;Waxman *et al.* 2009b;Koo *et al.* 2008;Koo *et al.* 2009). Such means to prevent the formation of α-syn polymerization are areas of intense investigation.

While *in vitro* studies provide important information regarding the function of α-syn and its role in PD, *in vivo* systems are required to further the investigation of therapeutics. α-Syn fibril formation is a nucleation-dependent process (Wood *et al.* 1999), and cellular seeding of amyloidogenic proteins has been previously observed (Ren *et al.* 2009). The current study presents the development and characterization of a novel, high-efficiency cellular model of α-syn aggregation, employing a combination of cellular seeding of α-syn polymerization and calcium phosphate precipitation. Using this system we examined the effects of single-point mutations as inhibitors of α-syn polymerization. This study provides an ideal model system, with which to investigate such potential inhibitors against α-syn amyloid formation.

MATERIALS AND METHODS

Expression and Purification of Recombinant α-Syn

The human α-syn cDNA was cloned into the Nde I and Hind III restriction sites of the bacterial expression vector pRK172. The pRK172 DNA construct expressing C-terminal truncated 1–120 α-syn (truncated at amino acid 120) was created by creating a premature stop-codon (Murray *et al.* 2003). The pRK172 DNA construct expressing N-terminal truncated 21–140 α-syn (with a Met codon added before amino acid 21) was generously provided by Dr. Virginia Lee (University of Pennsylvania, Philadelphia, PA). pRK172 plasmids expressing full-length α-syn with the mutations V66P, V66S, T72P or T75P were created with oligonucleotides corresponding to the amino acid substitutions by QuickChange site-directed mutagenesis (Stratagene, La Jolla, CA) of α-syn in pRK172. All mutations were confirmed by DNA sequencing. α-Syn proteins were expressed in E. coli BL21 (DE3) and purified as previously described (Giasson *et al.* 2001;Greenbaum *et al.* 2005).

Fibril Preparation of Recombinant α-Syn

For cellular experiments, α-syn proteins were assembled into filaments by incubation at 37°C at concentrations greater than 5 mg/ml in sterile phosphate buffered saline (PBS, Invitrogen) with continuous shaking at 1050 rpm (Thermomixer R, Eppendorf, Westbury, NY). Experimentation was planned so that α-syn would be visibly assembled (by filamentous clusters observed in the solution) by the day of cellular experimentation. α-Syn fibrils were diluted to a concentration of 1 mg/ml in sterile PBS and treated by water bath sonication for a minimum of 2 hours. In experiments where large fibrils were separated from small polymers, diluted fibrillized α-syn (prior to sonication) was centrifuged at 16,000 × *g* for 5 min, and the supernatant was removed and the pellet was re-suspended in sterile PBS. Protein concentrations of the original diluted fibrils and the supernatant were measured by BCA protein assay (Pierce). Concentration of the large fibrils was determined as the concentrations of [total - supernatant]. All samples were sonicated in a water bath prior to addition to cell culture media. Unless otherwise specified, cells were treated with 1 μM of recombinant 21–140 α-syn fibril mix.

Cell culture and transfection

QBI293 cells were maintained using Dulbecco's Modified Eagle's Medium (DMEM; Invitrogen) supplemented with 10% fetal bovine serum (FBS) and 1% penicillin/ streptomycin. SH-SY5Y cells stably expressing human wild-type (WT) α-syn were maintained as previously described (Mazzulli *et al.* 2006). The mammalian-expression vector pcDNA3.1 cloned with WT human α-syn cDNA was previously described (Paxinou *et al.* 2001). C-terminal truncated α-syn (1–120 α-syn) was created by the addition of a BamH1 restriction site directly prior to the stop codon of WT human α-syn in pcDNA3.1 using site using QuickChange site-directed mutagenesis (Stratagene). After which, this construct was digested with BamH1 and re-ligated back to itself without the insert. QuickChange site-directed mutagenesis was then used to remove extra base pairs to allow amino acid 120 to be followed by the already existing termination sequence and 3'-UTR region of WT α-syn in pcDNA3.1. The pcDNA3.1 constructs expressing full-length α-syn with the V66P, V66S, T72P or T75P mutations were created with oligonucleotides corresponding to the amino acid substitutions by QuickChange site-directed mutagenesis.

For experimentation, cells were plated onto 6-well plates and transfected at approximately 40% confluency, using calcium phosphate precipitation, as previously described, with minor modifications (Grant *et al.* 1997). pcDNA3.1 mammalian expression plasmid vectors containing the cDNA for the expression of α-syn protein (3 μg per 35 mm well) were diluted into $CaCl_2$ (0.5 M), for a total volume of 37.5 μl per 35 mm well. Experimentation using a single α-syn cDNA was performed with 1.5 μg of the α-syn DNA expression vector and 1.5 μg of pcDNA3.1 (empty vector). Experimentation with multiple cDNAs was performed with an equal proportion of each DNA expression vector. After mixing, the DNA/$CaCl_2$ mixture was added $1/5^{th}$ at a time into an equal volume of 2× BES buffer saline solution (50 mM *N*,*N*-bis(2-hydroxyethyl)-2-aminoethanesulfonic acid (BES), 280 mM NaCl, 1.5 mM Na_2HPO_4, pH 6.96), vortexing in between each addition, for a final volume of 75 μl of transfection solution per 35 mm well. Transfection solution was then incubated at room temperature for 15–20 min, after which it was added dropwise to media. Four hours after transfection, 1 μM (final concentration) of sonicated α-syn fibrils was added to the media, after which cells were incubated overnight at 37°C, 5% CO_2. In the current study, 28 ± 9% [SD] of QBI293 cells were transfected when treated with both calcium phosphate precipitation and recombinant fibrils (as assessed by SNL4 verses Hoechst immunoreactivity in 5 random experiments).

Approximately 16 hours after transfection, calcium phosphate was washed with PBS, and cells were trypsinized and replated onto poly-D-lysined plates or glass coverslips with warm DMEM containing 3% FBS and 1% penicillin/ streptomycin (reduced serum). SH-SY5Y neuroblastoma cells were washed with PBS and new media was replaced.

For the purpose of experimentation, the time of the media change was considered “Time 0.” Cells were harvested or fixed 48 hours after Time 0, except where otherwise specified.

Biochemical cellular fractionation

Cells were washed one time in ice-cold PBS, and samples were harvested in 25 mM Tris-HCl, pH 7.5, 150 mM NaCl, 1 mM EDTA, 1% Triton X-100, 20 mM NaF, and a cocktail of protease inhibitors containing 1 mM phenylmethylsulfonyl and 1 mg/ml each of pepstatin, leupeptin, N-tosyl-L-phenylalanyl chloromethyl ketone, N-tosyl-lysine chloromethyl ketone and soybean trypsin inhibitor. Samples were sedimented at 100,000 × *g* for 30 min at 4°C. Supernatants were removed and pellets were sonicated in 1.5× Laemmli sample buffer. 5× SDS sample buffer was added and samples were heated to 100°C for 5 min prior to Western blot analysis. Equal proportions of supernatant (triton-soluble protein) and pellet (triton-insoluble protein) were loaded and analyzed as percent pelleted.

Antibodies

Syn211 is a mouse monoclonal antibody specific for human α-syn, requiring amino acids 121–125 (Giasson *et al.* 2000). SNL4 is a polyclonal rabbit antibody raised against a synthetic peptide corresponding to amino acids 2–12 of α-syn (Giasson *et al.* 2000). SNL4 recognizes all LBs and GCIs in cases of PD, DLB, and MSA (Duda *et al.* 2000;Giasson *et al.* 2000). Syn514 is a mouse monoclonal antibody, which preferentially recognizes pathological α-syn (Duda *et al.* 2002;Waxman *et al.* 2008). pSer129 is a mouse monoclonal antibody that specifically recognizes α-syn phosphorylated at Ser129 (Waxman and Giasson 2008). Additional antibodies include anti-ubiquitin (Sigma-Aldrich, St. Louis, MO), anti-vimentin (Sigma-Aldrich), anti-lamp1 (BD Biosciences, San Jose, CA), anti-γ-tubulin (Sigma-Aldrich), anti-β-tubulin (Sigma-Aldrich), anti-mannosidase II (Chemicon), and anti-calnexin (Cell Signaling Technology).

Western blot analysis

Protein samples were resolved by SDS-PAGE on 15% polyacrylamide gels, followed by electrophoretic transfer onto nitrocellulose membranes. Membranes were blocked in Tris buffered saline (TBS) with 5% dry milk, and incubated overnight with SNL4 or Syn211 in TBS/ 5% dry milk or pSer129 in TBS/ 5% bovine serum albumin (BSA). Each incubation was followed by goat anti-mouse conjugated horseradish peroxidase (HRP) (Amersham Biosciences, Piscataway, NJ) or goat anti-rabbit HRP (Cell Signaling Technology, Danvers, MA), and immunoreactivity was detected using chemiluminescent reagent (NEN, Boston, MA) followed by exposure onto X-ray film.

Cell culture immunofluorescence

Double-immunofluorescence of transfected cells was completed as previously described (Mazzulli *et al.* 2006;Waxman *et al.* 2009a). Cells were fixed at −20°C with 100% MeOH for 20 min, followed by 50% MeOH and 50% acetone for 5 min. For Thioflavin S immunostaining, coverslips were fixed in 4% paraformaldehyde for 8 minutes, followed by PBS / 0.1% Triton X-100 for 10 min. Following washes with PBS, coverslips were blocked with PBS containing 5% bovine serum albumin (BSA), and primary antibodies were diluted into blocking solution for 1–2 h at room temperature. Following PBS washes, coverslips were incubated in secondary antibodies conjugated to Alexa 488 or Alexa 594 [Mouse IgG,

Mouse IgG_{2A} (for pSer129), Mouse IgG_1 (for Syn514, anti-γ-tubulin, anti-vimentin, anti-ubituiqin, anti-β-tubulin, and anti-mannosidase II), or Rabbit IgG] for 1 h. Thioflavin S (Sigma-Aldrich) immunostaining was performed after secondary antibody incubation at a concentration of 0.05%, after which coverslips were washed three times in 70% ethanol followed by washes in water. Nuclei were counterstained with Hoechst trihydrochloride trihydrate 33342 (Invitrogen), and coverslips were mounted using Fluoromount-G (Southern Biotech, Birmingham, AL).

Fluorescence microscopy

Immunofluorescence was captured on an Olympus BX51 fluorescence microscope mounted with a DP71 digital camera (Olympus, Center Valley, PA). Cellular co-localization images were captured on a Zeiss Axiovert 200M inverted confocal microscope mounted with a Zeiss LSM510 META NLO digital camera utilizing Zeiss LSM510 META V3.2 confocal microscope software (Zeiss, Thornwood, NY). Confocal images were captured with 63× oil optics, and all representative images were of one Z-plane of <0.7 μm.

Filament Assembly and Centrifugal Sedimentation

α-Syn proteins were assembled into filaments by incubation at 37°C in 100 mM sodium acetate, pH 7.4 with continuous shaking at 1050 rpm (Thermomixer R, Eppendorf). A fraction of each sample was set aside for K114 and Thioflavin T (ThT) fluorometry and electron microscopic (EM) analysis. The remainder of each sample was centrifuged at 100,000 × *g* for 20 min. SDS-sample buffer (10 mM Tris, pH 6.8, 1 mM EDTA, 40 mM DTT, 1% SDS, 10% sucrose) was added to pellets and supernatants, which were heated to 100°C for 15 min. Equal volumes of α-syn proteins in the supernatants and pellets were separated by SDS-PAGE and were quantified by densitometry of Coomassie Blue R-250 stained gels.

K114 and ThT Fluorometry

α-Syn fibrils are amyloidogenic (Conway *et al.* 2000) and their formation can be quantified using the fluorescent amyloid binding dye K114 or ThT (Crystal *et al.* 2003;Conway *et al.* 2000). K114 is derived from the structure of Congo Red and demonstrates a tremendous increase in fluorescence in solution assays upon binding to amyloidogenic fibrils (Crystal *et al.* 2003). This assay was conducted, as previously described (Crystal *et al.* 2003), by incubating a fraction of each sample with the K114 (50 μM) in 100 mM glycine, pH 8.6 and measuring fluorescence (λ_{ex}=380 nm, λ_{em}=550 nm, cutoff = 530 nm) with a SpectraMax Gemini fluorometer and SoftMax Pro 4.0 software. ThT fluorometry was performed using ThT (20 μM) diluted into 100 mM glycine, pH 8.0 using the follow parameters: λ_{ex}=450 nm, λ_{em}=482 nm, cutoff = 475 nm.

Negative Staining EM

Assembled α-syn filaments were absorbed onto 300 mesh carbon coated copper grids, stained with 1% uranyl acetate and visualized with a JEOL 1010 transmission electron microscope (Peabody, MA). Images were captured with a Hamamatsu digital camera (Bridgewater, MA) using AMT software (Danvers, MA).

Quantitative analysis

Western blot data were quantified by ImageJ software (NIH, Bethesda, MD). Data were analyzed as a change of percent pelleted from vehicle control conditions. Cells were counted by capture and counting of 3–6 random fields per experiment. All comparisons were completed by two-way, parametric t-tests using GraphPad InStat software (San Diego, CA). Each experiment was performed a minimum of three times.

RESULTS

Recombinant, fibrillized α-syn can seed intracellular α-syn aggregation

Although many studies have examined α-syn aggregates in cellular model systems, current cellular models have been limited in providing abundant α-syn aggregates that adequately display the major features of pathological brain inclusions (Lee *et al.* 2004;Smith *et al.* 2005;Fornai *et al.* 2004;O'Farrell *et al.* 2001;Pandey *et al.* 2006;Tsuchiya *et al.* 2005;Zhou and Freed 2004). Many cell models present small α-syn aggregates, or often only a low percentage of cells (normally between 2 and 15%) exhibit large aggregates, which share several characteristics with pathological inclusions. While these models can provide useful information, we sought to develop a new high-efficiency model cell system that produced aggregates with characteristics similar to authentic inclusions. In developing a new model cell system, we had many goals. A major objective of an ideal model is to study the formation or the prevention of large, cellular aggregates both by Western blot analyses and by broad visualization with immunofluorescence. Further, we wanted to avoid tags that may alter the properties of α-syn. We also did not want to depend on stable, overexpression cell lines, which may exhibit altered properties due to selection and could limit experimental manipulation. Through serendipitous experimental testing, we found that a combination of calcium phosphate precipitation (Grant *et al.* 1997) and cellular uptake of sonicated, recombinant-generated α-syn fibrils (Lee *et al.* 2008) to act as a nucleus for α-syn aggregation provided us with an ideal cellular system.

QBI293 cells were transiently transfected by calcium phosphate precipitation with plasmids for the expression WT α-syn, after which recombinant, pre-fibrillized, sonicated WT α-syn was added to the media (as described in “Materials and Methods”). Within 24 hours after the removal of the calcium phosphate precipitant, the normally diffuse, cytosolic immunoreactivity of intracellular α-syn (in the absence of fibril treatment; Figure 1A), was replaced by abundant, large cellular aggregates (Figure 1B, arrows). However, immunoreactivity of the exogenous α-syn fibrils was also observed with an anti-α-syn antibody (SNL4). These exogenous fibrils clustered on the outside of cells, partially obscuring the visibility of aggregates (arrows) and endogenous, soluble protein (arrowhead). α-Syn is hyperphosphorylated at Ser129 in animal models and human disease (Fujiwara *et al.* 2002;Kahle *et al.* 2002;Anderson *et al.* 2006;Nishie *et al.* 2004;Neumann *et al.* 2002;Waxman and Giasson 2008). We therefore, used an antibody specific for phospho-Ser129 of α-syn (pSer129) to detect specifically intracellular aggregates, which were robustly immunoreactive. By confocal microscopy, pSer129 recognized large fibrous, intracellular aggregates that sometimes appeared with a hollow core and displaced or circled the nuclear membrane. Further, they were thioflavin S positive (Figure 1C), but thioflavin also strongly identified punctae inside and around the cell, consistent with the exogenous, recombinant fibrils. We aimed to discern between endogenously expressed α-syn and recombinant, exogenous fibril treatment to further analyze the composition and formation of these cellular aggregates. To do so, we took advantage of C- or N-terminally truncated α-syn and utilized epitope-specific antibodies to these regions (Figure 1D).

QBI293 cells were transiently transfected by calcium phosphate precipitation with plasmids expressing either WT or C-terminally truncated 1–120 α-syn, after which recombinant, pre-fibrillized, sonicated α-syn (WT, 1–120, or 21–140 α-syn) was added to the media. In cells endogenously expressing WT α-syn with the addition of recombinant 1–120 α-syn fibrils, antibody SNL4 intensely recognized large α-syn aggregates that were robustly pSer129 immunoreactive, indicating that these aggregates contained endogenously expressed WT α-syn. SNL4 also recognized punctae inside and around cells, consistent with detection of the 1–120 α-syn recombinant fibrils (Figure 2A). Cells that were transfected with the 1–120 α-syn expression plasmid and then treated with recombinant WT α-syn fibrils were only

sparsely pSer129 immunoreactive (Figure 2B), indicating that phosphorylation of exogenous recombinant α-syn protein fibrils was minimal and/or that exogenously added α-syn fibrils comprised only a minor component of the intracellular aggregates. Cells were then transfected with the WT α-syn expression plasmid and were treated with recombinant 21–140 α-syn fibrils. Under these conditions, intracellular α-syn aggregates were robustly detected with SNL4 and pSer129 antibodies (Figure 2C,D). Non-aggregated, cytoplasmic, endogenously expressed α-syn immunoreactivity with SNL4 could be observed concurrently in cells with small aggregates (Figure 2C, arrowheads), prior to the development of large, fibrous aggregates (Figure 2C, arrow; 2D). Syn514 specifically recognized the protein aggregates and showed 100% co-localization with pSer129 immunoreactivity (Fig. 2E,F), consistent with the conformational specificity of this antibody (Waxman *et al.* 2008). These findings support the recruitment of mostly endogenously expressed α-syn into these large cellular aggregates, irrespective of WT or truncated α-syn species either endogenously expressed or used for recombinant fibril treatment.

Biochemical fractionation and Western blot analyses further supported the formation of triton-insoluble α-syn aggregates, primarily composed of endogenously-expressed protein (Figure 3). We further isolated subpopulations of α-syn polymers to examine the requisite fibril population for intracellular aggregate formation. Cells were treated with recombinant, soluble α-syn, a fibril mix (total protein after *in vitro* fibrillization, as utilized above), isolated large fibrils, or small fibrils/soluble protein. Triton-soluble α-syn was observed with SNL4 (Figure 3A) and Syn211 (data not shown) in all conditions. The presence of triton-insoluble WT α-syn was observed with SNL4, Syn211, and pSer129 for all conditions treated with recombinant, fibrillized α-syn (Figure 3B–D). However, 0.1 μM of large fibrils performed similarly to 1 μM of total fibril mix, with 1 μM of small fibrils/polymers/soluble protein performing less efficiently. Minimal triton-insoluble α-syn was observed when cell cultures were treated with soluble, native recombinant α-syn.

Consistent with antibody-specificity, SNL4 recognized both WT α-syn and recombinant, fibrillized 1–120 α-syn in the triton-insoluble fraction, but Syn211 only detected WT α-syn. pSer129 identified intracellular, triton-insoluble WT α-syn, and only negligible immunoreactivity of soluble WT α-syn protein was observed with pSer129 (with over-exposure – data not shown). Higher molecular weight species of WT α-syn were further observed in the triton-insoluble fraction, consistent with ubiquitination of α-syn (Sampathu *et al.* 2003). Recombinant, fibrillized 21–140 α-syn immunoreactivity was often not observed with either Syn211 or pSer129 antibodies, suggesting that the amount of recombinant, fibrillized proteins that were internalized to promote aggregate formation was minimal and/or that these proteins may be subject to degradation.

The most consistent and efficient treatment condition was that of WT α-syn DNA transfection with the addition of the recombinant 21–140 α-syn fibril mix. After 48 hours (after calcium phosphate precipitation removal), 77 ± 15% [SD] (n = 5) of transfected cells, as assessed by SNL4 immunofluorescence, contained pSer129 immuno-positive aggregates. The aggregates were first readily observed by Western blot at 24 hours after calcium phosphate precipitation removal, where 19 ± 16% [SD] of total, endogenous protein appeared in the triton-insoluble fraction (Figure 4A). By 48 hours, 49 ± 5% [SD] of total, endogenous α-syn was observed in the triton-insoluble fraction, which increased to 65 ± 17% [SD] at 72 hours (n = 3).

The role of calcium phosphate precipitation on aggregate formation in SH-SY5Y neuroblastoma

Recent studies have supported membrane-mediated cellular uptake of α-syn (Liu *et al.* 2009;Ahn *et al.* 2006;Lee *et al.* 2005;Lee *et al.* 2008), and translocation of α-syn into SH-

SY5Y neuroblastoma can cause aggregate formation (Desplats *et al.* 2009). We therefore examined what role, if any, calcium phosphate precipitation played in the formation of α-syn aggregates by treating SH-SY5Y neuroblastoma that were stably transfected with WT α-syn with the recombinant 21–140 α-syn fibril mix. In the absence of transfection, no increase in triton-insoluble, endogenously expressed α-syn was observed over that of cells that did not receive fibril treatment (Figure 4B). SH-SY5Y neuroblastoma that were treated with calcium phosphate precipitation using an empty vector plasmid (pcDNA3.1), followed by fibril treatment, produced triton-insoluble WT α-syn that was also pSer129 immunoreactive. To control for effects of calcium phosphate precipitation, cells were treated with calcium phosphate and the precipitant was washed off prior to the addition of fibrils. This treatment precluded the increased triton-insoluble α-syn that was observed by Western blot analysis when both calcium phosphate precipitation and fibrils were concurrently present.

Double-immunofluorescence on SH-SY5Y neuroblastoma revealed relative changes in the abundance of large aggregate formation. In the absence of fibril treatment, there was a paucity of pSer129 or SNL4 positive aggregates (Figure 5A). With calcium phosphate precipitation and fibril addition, 12 ± 7% [SD] of neuroblastoma formed aggregates ($p = 0.001$; Figure 5B). Similar to QBI293 cells, large α-syn-containing, highly phosphorylated, fibrous aggregates were observed by confocal microscopy (Figure 5E). However, small increases in aggregate formation were also observed in the absence of calcium phosphate precipitation or with calcium phosphate removal prior to fibril addition (Figure 5C,D). In each condition, 2 ± 1% [SD] of neuroblastoma formed large aggregates, greater than that of no fibril addition ($p = 0.001$ and $p = 0.0003$, respectively), but less than treatments including calcium phosphate precipitation ($p = 0.005$ and $p = 0.003$, respectively; $n = 7$ for all conditions). Therefore, although fibrils can enter cells through membrane translocation, our data suggest that this process is inefficient in the absence of calcium phosphate precipitation.

α-Syn intracellular aggregates are ubiquitinated and independent from cytoskeletal markers

We further characterized these α-syn aggregates by performing double-immunofluorescence between pSer129, a specific marker for intracellular α-syn aggregates, and multiple cellular markers. A subset of aggregates was strongly immunopositive for ubiquitin (Supplemental Figure 1A). This observation is consistent with human brain samples, in which only a subset of α-syn pathological inclusions are positive for ubiquitin (Sampathu *et al.* 2003). α-Syn aggregates did not co-localize with cytoskeletal markers γ-tubulin, β-tubulin, or vimentin (Supplemental Figure 1B–D). However, the aggregate often surrounded the γ-tubulin-positive centrosome (B, arrows), and γ-tubulin immunoreactivity was often reduced in aggregate-containing cells. β-Tubulin and vimentin appeared normal, but were displaced from perinuclear areas. Lamp1 surrounded and, in some cases, was trapped inside the fibrous aggregate (Supplemental Figure 1E). In many cells with aggregates, lamp1 was abnormally enlarged (arrowheads), suggesting reactive lysosomes. However, these lysosomes were not positive for pSer129 immunoreactivity. Ultrastructure analyses demonstrated that the α-syn aggregates were cytoplasmic and comprised of a fibrillar network (Supplemental Figure 2). These aggregates were often in perinuclear areas and were not membrane bound.

Analysis of single-point mutations in the hydrophobic region that inhibit α-syn fibril formation

Our novel cellular model of α-syn aggregation allows for a wide variety of manipulation due to the nature of transient transfections. We, therefore, sought to identify alterations in α-syn that might block the formation of these aggregates. The middle hydrophobic region of α-syn plays a critical role in amyloid formation (Giasson *et al.* 2001;Waxman *et al.* 2009b;Zibaee

et al. 2007), and recent studies have identified single-point mutations in this region that abrogate fibril formation *in vitro* (Koo *et al.* 2008;Koo *et al.* 2009). We selected four of the mutants (V66P, V66S, T72P, and T75P) to examine in our cellular model.

Prior to cellular experimentation, we independently examined the ability of these four single-point mutations to inhibit α-syn fibril formation, *in vitro*. Recombinant generated WT α-syn or α-syn containing each of these point mutations was incubated under *in vitro* assembly conditions at a concentration of 5 mg/ml and then analyzed after 2, 4, and 9 days by four different methods: ThT fluorometry, K114 fluorometry, quantitative sedimentation, and EM analysis. Similar to previous reports (Koo *et al.* 2008;Koo *et al.* 2009), all four mutant proteins demonstrated impaired fluorometry following incubation when compared to WT α-syn (Figure 6A). However, some increased ThT fluorometry was observed for V66S α-syn. For this mutant, significantly increased K114 fluorometry and sedimentation were also observed, but the sedimentation rate was reduced relative to WT α-syn (Figure 6B,C). The V66P, T72P and T75P mutants did not produce a K114 fluorescence signal or form large polymers that could be sedimented.

By EM analysis the V66P and T72P proteins only formed small, often circular, aggregates of varying sizes ranging from 10 to 40 nm in diameter (Supplemental Figure 3B for V66P; data not shown for T72P), while V66S α-syn formed extended fibrils that usually formed parallel bundles and appeared ribbon-like (Supplemental Figure 3C). These were quite different from the typically negatively stained α-syn fibrils that are curvilinear and distributed in a random pattern (Supplemental Figure 3A). T75P α-syn did not polymerize into fibrils, but developed small aggregates of diverse shape and structure (Supplemental Figure 3D).

After verifying that three of single-point mutations significantly prevent α-syn fibril formation, *in vitro*, QBI293 cells were transfected with the expression plasmids of each of these mutant α-syn proteins, and then cells were treated with recombinant 21–140 α-syn fibrils. Using biochemical fractionation, followed by Western blot analysis, only WT and V66S α-syn proteins were consistently observed in the triton-insoluble fractions (Figure 7A). However, in one instance (n = 5), a trace increase of T75P α-syn was observed in the triton-insoluble fraction (Figure 7A, asterisk). Double-immunofluorescence on cells transfected with the plasmids for the expression of V66P α-syn or T72P α-syn and then treated with recombinant fibrils identified small, infrequent aggregates with pSer129 immunostaining (Figure 7B,C; arrows). In contrast, there was a paucity of pSer129 or SNL4 positive aggregates in cells transfected with the T75P α-syn expression plasmid and treated with recombinant fibrils (Figure 7D). Cells transfected with the V66S α-syn expression plasmid and treated with recombinant fibrils revealed pSer129 and SNL4 positive aggregates (Figure 7E) similar to those in cells expressing WT α-syn.

Single-point mutations V66S, V66P, T72P, and T75P have been reported to not only be deficient in amyloid formation, but also be capable of inhibiting amyloid formation of WT α-syn under *in vitro* co-assembly conditions (Koo *et al.* 2009). To independently assess the ability of these proteins to inhibit WT α-syn under our conditions, recombinant generated V66P, V66S, T72P, and T75P mutant α-syn proteins were co-incubated *in vitro* with recombinant WT α-syn, each at a concentration of 2.5 mg/ml for 4 days and analyzed by ThT fluorometry, K114 fluorometry, quantitative sedimentation, and EM analysis. At odds with previous reports, co-incubation of WT α-syn with either V66P or T72P α-syn did not block amyloid formation (Figure 8). Only V66S and T75P α-syn mutations significantly reduced ThT fluorescence, when compared to WT α-syn alone (2.5 mg/ml; Figure 8A). However, inhibition with V66S α-syn was not observed by K114 fluorometry (Figure 8B), and only a modest reduction in sedimentation was noted (Figure 8C). In contrast, T75P α-

syn significantly reduced ThT and K114 fluorescence, and significantly reduced the amount of sedimented protein. In addition, increasing the concentration of T75P α-syn to 5 mg/ml under co-assembly conditions caused a further reduction in ThT and K114 fluorometry. Other mutations at a concentration of 5 mg/ml did not significantly reduce these measures of amyloid formation under co-assembly conditions (data not shown).

By EM, V66P with WT α-syn and T72P with WT α-syn formed highly bundled fibrils with dominant positive stain (Supplemental Figure 4A,B). V66S with WT α-syn formed a mixture of polymers, some of which appeared filamentous with a negatively stained pattern, while the majority was a positively stained lattice network consistent with some level of non-specific protein aggregation (Supplemental Figure 4C). T75P with WT α-syn, on the other hand, created short aggregates of varying shapes and sizes (Supplemental Figure 4D), similar to those observed with T75P α-syn alone. However, these aggregates appeared larger in size, consistent with the modest increase in sedimentation of α-syn proteins under these conditions.

To examine the ability of these single-point mutations to inhibit the formation of WT α-syn cellular aggregates, QBI293 cells were co-transfected with plasmids for the expression of WT α-syn and α-syn containing each one of the single-point mutations. Co-transfection with the WT α-syn expression plasmid and an empty vector pcDNA3.1 (pcDNA) was also performed as a control (WT only). While all mutant α-syn proteins increased the amount of soluble α-syn observed by Western blot analysis (Figure 9A), all conditions produced comparable amounts of triton-insoluble α-syn (n = 4 for P mutations and n = 3 for V66S). Similarly, aggregate formation was not distinguishable from WT α-syn transfection alone by double-immunofluorescence with SNL4 and pSer129 (Figure 9B–D; data not shown for WT/V66P α-syn and WT/T72P α-syn). Therefore, although the V66P, T72P and T75P single-point mutations were capable of significantly impairing the formation of α-syn cellular aggregates on their own, they were not able to inhibit amyloid formation by expression of WT α-syn in our cellular model.

DISCUSSION

Intracellular α-syn amyloidogenic inclusions are a characteristic pathological hallmark of PD, among other diseases, and factors that prevent or decrease the development of these proteinaceous aggregates are areas of intense investigation. While *in vitro* systems are informative, the cellular milieu needs to be considered for potential therapeutic intervention. The current study presents a novel cellular model for the study of α-syn amyloid formation. This model provides the availability for unique experimentation, since approximately half of all endogenously expressed α-syn protein was recruited into large cellular aggregates after 48 hours. Therefore, both large and small changes in aggregate formation could by evaluated quantitatively by Western blot analysis. Further, the ability to form cellular aggregates appeared only limited by the transfection efficiency mediated by calcium phosphate precipitation. After 48 hours, an average of 77% of QBI293 transfected cells and 12% of SH-SY5Y neuroblastoma presented with large cellular aggregates with similar characteristics to pathological inclusions in human brains. This suggests that most cells that internalize DNA during calcium phosphate-mediated transfection also internalize exogenous α-syn fibrils. Although treatment of cell cultures with recombinant α-syn fibrils without calcium phosphate precipitation can induce the formation of large α-syn aggregates in cells, this process is not efficient. Calcium phosphate-DNA precipitants likely promote the entry of α-syn polymers into the cytoplasm of cells, providing an ideal system for the study of α-syn amyloid formation in the presence of the cellular milieu.

The cellular aggregates described herein further shared the biochemical properties of human pathological inclusions such as hyperphosphorylation at Ser129, ubiquitination, and insolubility to triton X-100. These inclusions were also amyloidogenic and comprised of cytoplasmic filamentous bundles that were not membrane bound, indicating that they were not lysosomal, autophagic, or contained in any organelle. Further, they were independent of cytoskeletal structures, displacing them rather than co-localizing with them. Some cellular models of α-syn aggregation suggest that α-syn forms aggresomes (Opazo *et al.* 2008;Ardley *et al.* 2004;Hasegawa *et al.* 2004;Lee *et al.* 2002). The α-syn aggregates presented here did not co-localize with characteristic aggresome cellular markers (Garcia-Mata *et al.* 1999;Waelter *et al.* 2001;Johnston *et al.* 1998) and were therefore not aggresomes, in agreement with another recently published cellular model of α-syn aggregate formation (Luk *et al.* 2009), and consistent with pathological inclusions observed in human brain (Nedelsky *et al.* 2008).

To avoid the use of bulky tags, which may alter the propensity of protein to aggregate and potentially affect other properties, we utilized epitope-specific antibodies, truncated recombinant α-syn protein, and a phospho-specific antibody to Ser129 α-syn to distinguish intracellular protein from that potentially sticking to the outside of the cell. These modifications allowed us to examine the internalization of α-syn that has been observed by others (Desplats *et al.* 2009;Lee *et al.* 2008) and the formation of intracellular protein aggregates primarily composed of endogenously expressed α-syn. Interestingly, initial investigation of recombinant C-terminal and N-terminal truncated α-syn as the nuclei for cellular aggregate formation identified 21–140 α-syn as more effective. This is counter intuitive, since 21–140 α-syn fibrillizes at a slower rate than WT α-syn (Zibaee *et al.* 2007), and 1–120 α-syn is more accelerated, *in vitro* (Murray *et al.* 2003). 21–140 α-syn may be more effective at seeding than 1–120 α-syn, *in vivo*. On the other hand, the removal of membrane binding domains in the N-terminus (Perrin *et al.* 2000;Bisaglia *et al.* 2006) may allow more protein to be available for seeding, rather than sequestered in membrane associations. Despite differences in relative efficiency, 1–120, 21–140, and WT α-syn recombinant fibrils were all capable of promoting cellular aggregate formation.

This novel system allowed us to examine single-point mutations in the hydrophobic residue on the ability of α-syn to form cellular aggregates to complement *in vitro* investigations. Mutant proteins V66P, T72P, and T75P significantly impeded the formation of α-syn cellular aggregation, similar to *in vitro* experimentation using recombinant α-syn protein. The finding that these single-point mutations responded to aggregate formation similar to *in vitro* fibrillization provides additional validity to our model. However, the T75P mutation, which significantly inhibited the ability of WT α-syn to form amyloid *in vitro*, could not prevent the formation of WT α-syn cellular aggregates. Our studies suggest that this cellular model is more efficient at promoting amyloid formation than similar studies *in vitro*. The rate of α-syn aggregation is increased in the presence of a nucleus (Wood *et al.* 1999), and the cellular environment may accelerate nucleation of amyloidogenic proteins (Zhou *et al.* 2009). The cellular milieu provides an environment concentrated in protein, nucleic acids, and carbohydrates, which may subject α-syn to macromolecular crowding, thereby accelerating α-syn fibrillization (Uversky *et al.* 2002). This increased propensity for amyloid formation or other cellular components may prevent effective inhibition of WT α-syn aggregation using the means utilized in the current study.

In the process of validating the single-point mutations examined in this study, we identified disparities between our *in vitro* results and those previously reported (Koo *et al.* 2008;Koo *et al.* 2009), which may be due in part to differences in experimental conditions. The V66S mutant protein, although significantly impeding ThT fluorescence, demonstrated elevated K114 fluorescence and could polymerize into long filamentous polymers with altered

morphology. This mutation appears to alter the structure of α-syn within fibrils, which may directly inhibit ThT binding or alter the typical conformation required for ThT recognition without affecting binding to K114, which is structurally derived from Congo Red (Crystal *et al.* 2003). Reactivity to the fluorescent dyes Congo Red and ThT are characteristic defining properties of amyloid formation (Glenner 1980); however, the binding sites for these two molecules are believed to be mutually exclusive (Klunk *et al.* 1989;Zhuang *et al.* 2001). Our results indicate that the use of both measures provides a more accurate evaluation of amyloid formation *in vitro*.

Additionally, although ultrastructural changes were observed, V66P and T72P α-syn did not significantly inhibit the amyloid formation of WT α-syn, and co-incubation of WT α-syn with V66S α-syn inhibited ThT fluorometry, but not K114 fluorometry. EM analysis revealed that co-incubation of V66S and WT α-syn resulted in a mixture of polymers some of which appeared filamentous with a negatively stained pattern, while the majority was a positively stained lattice network consistent with some level of non-specific protein aggregation. Interestingly, the co-assembly of both proteins resulted in polymers that differ from those of either protein individually. This finding indicates that modifications in amino acid structure can alter the morphology of amyloid fibrils in manners beyond prediction, but even with these major structural changes, α-syn has a driving propensity to still form amyloid.

The recent discovery that α-syn is capable of membrane translocation and recycling (Liu *et al.* 2009;Ahn *et al.* 2006) and that fibrillized α-syn may be transferred between neurons (Lee *et al.* 2008;Desplats *et al.* 2009) has provided a new vantage point on α-syn pathology. The current study not only provides a novel, high-efficiency model of aggregate formation, but also provides a tool that can be accomplished with common laboratory reagents, rather than requiring expensive kits, the generation of stable cell lines, or multiple, confounding manipulations. Further, the formation of α-syn aggregates in cultured cells in the current study may equate to cross-membrane transmission of neuronal inclusions in human patients that have received neuronal transplants (Kordower *et al.* 2008;Li *et al.* 2008;Desplats *et al.* 2009). Our use of calcium phosphate precipitation serves as a useful tool, providing the additional efficiencies required for identifying potential therapeutic strategies. Relative differences between *in vitro* and *in vivo* measures using α-syn mutant proteins further underscore the need for such models. A better understanding of basic molecular requirements, in combination with cellular factors involved in α-syn inclusions formation, will provide further insights that may enable the generation of therapeutic agents capable of preventing the assembly of cellular aggregates.

Supplementary Material

Refer to Web version on PubMed Central for supplementary material.

Acknowledgments

This work was funded by grants from the National Institute on Aging (AG09215) and the National Institute of Neurological Disorders and Stroke (NS053488). E.A.W. was supported by a training grant (T32 AG00255) from the National Institute on Aging. We thank the Biochemical Imaging Core Facility supported by Abramson Cancer Institute at the University of Pennsylvania for assistance in the EM and confocal microscopy studies.

REFERENCES

Ahn KJ, Paik SR, Chung KC, Kim J. Amino acid sequence motifs and mechanistic features of the membrane translocation of alpha-synuclein. J. Neurochem. 2006; 97:265–279. [PubMed: 16524375]

Anderson JP, Walker DE, Goldstein JM, et al. Phosphorylation of Ser-129 is the dominant pathological modification of alpha-synuclein in familial and sporadic Lewy body disease. J. Biol. Chem. 2006; 281:29739–29752. [PubMed: 16847063]

Ardley HC, Scott GB, Rose SA, Tan NG, Robinson PA. UCH-L1 aggresome formation in response to proteasome impairment indicates a role in inclusion formation in Parkinson's disease. J. Neurochem. 2004; 90:379–391. [PubMed: 15228595]

Biere AL, Wood SJ, Wypych J, et al. Parkinson's disease-associated alpha-synuclein is more fibrillogenic than β- and γ-synuclein and cannot cross-seed its homologs. J. Biol. Chem. 2000; 275:34574–34579. [PubMed: 10942772]

Bisaglia M, Schievano E, Caporale A, Peggion E, Mammi S. The 11-mer repeats of human alpha-synuclein in vesicle interactions and lipid composition discrimination: a cooperative role. Biopolymers. 2006; 84:310–316. [PubMed: 16411187]

Conway KA, Harper JD, Lansbury PT. Accelerated in vitro fibril formation by a mutant alpha-synuclein linked to early-onset Parkinson disease. Nat. Med. 1998; 4:1318–1320. [PubMed: 9809558]

Conway KA, Harper JD, Lansbury PT. Fibrils formed in vitro from alpha-synuclein and two mutant forms linked to Parkinson's disease are typical amyloid. Biochemistry. 2000; 39:2552–2563. [PubMed: 10704204]

Crystal AS, Giasson BI, Crowe A, Kung MP, Zhuang ZP, Trojanowski JQ, Lee VM. A comparison of amyloid fibrillogenesis using the novel fluorescent compound K114. J. Neurochem. 2003; 86:1359–1368. [PubMed: 12950445]

Desplats P, Lee HJ, Bae EJ, Patrick C, Rockenstein E, Crews L, Spencer B, Masliah E, Lee SJ. Inclusion formation and neuronal cell death through neuron-to-neuron transmission of alpha-synuclein. Proc. Natl. Acad. Sci U. S. A. 2009; 106:13010–13015. [PubMed: 19651612]

Du HN, Tang L, Luo XY, Li HT, Hu J, Zhou JW, Hu HY. A peptide motif consisting of glycine, alanine, and valine is required for the fibrillization and cytotoxicity of human alpha-synuclein. Biochemistry. 2003; 42:8870–8878. [PubMed: 12873148]

Duda JE, Giasson BI, Gur TL, et al. Immunohistochemical and biochemical studies demonstrate a distinct profile of alpha-synuclein permutations in multiple system atrophy. J. Neuropathol. Exp. Neurol. 2000; 59:830–841. [PubMed: 11005264]

Duda JE, Giasson BI, Mabon ME, Lee VMY, Trojanoswki JQ. Novel antibodies to synuclein show abundant striatal pathology in Lewy body diseases. Ann. Neurol. 2002; 52:205–210. [PubMed: 12210791]

Forman MS, Lee VM, Trojanowski JQ. Nosology of Parkinson's disease: looking for the way out of a quackmire. Neuron. 2005; 47:479–482. [PubMed: 16102530]

Fornai F, Lenzi P, Gesi M, et al. Methamphetamine produces neuronal inclusions in the nigrostriatal system and in PC12 cells. J. Neurochem. 2004; 88:114–123. [PubMed: 14675155]

Fujiwara H, Hasegawa M, Dohmae N, Kawashima A, Masliah E, Goldberg MS, Shen J, Takio K, Iwatsubo T. α-Synuclein is phosphorylated in synucleinopathy lesions. Nat. Cell Biol. 2002; 4:160–164. [PubMed: 11813001]

Garcia-Mata R, Bebok Z, Sorscher EJ, Sztul ES. Characterization and Dynamics of Aggresome Formation by a Cytosolic GFP-Chimera. J. Cell Biol. 1999; 146:1239–1254. [PubMed: 10491388]

Giasson BI, Jakes R, Goedert M, Duda JE, Leight S, Trojanowski JQ, Lee VMY. A panel of epitope-specific antibodies detects protein domains distributed throughout human alpha-synuclein in Lewy bodies of Parkinson's disease. J. Neurosci. Res. 2000; 59:528–533. [PubMed: 10679792]

Giasson BI, Murray IVJ, Trojanowski JQ, Lee VMY. A hydrophobic stretch of 12 amino acid residues in the middle of alpha-synuclein is essential for filament assembly. J. Biol. Chem. 2001; 276:2380–2386. [PubMed: 11060312]

Giasson BI, Uryu K, Trojanowski JQ, Lee VMY. Mutant and wild type human alpha-synucleins assemble into elongated filaments with distinct morphologies in vitro. J. Biol. Chem. 1999; 274:7619–7622. [PubMed: 10075647]

Glenner GG. Amyloid deposits and amyloidosis. N. Engl. J. Med. 1980; 302:1283–1292. [PubMed: 6154243]

Goedert M. Alpha-synuclein and neurodegenerative diseases. Nat. Rev. Neurosci. 2001; 2:492–501. [PubMed: 11433374]

Grant ER, Bacskai BJ, Pleasure DE, Pritchett DB, Gallagher MJ, Kendrick SJ, Kricka LJ, Lynch DR. N-Methyl-D-aspartate Receptors Expressed in a Nonneuronal Cell Line Mediate Subunit-specific Increases in Free Intracellular Calcium. J. Biol. Chem. 1997; 272:647–656. [PubMed: 8995308]

Greenbaum EA, Graves CL, Mishizen-Eberz AJ, Lupoli MA, Lynch DR, Englander SW, Axelsen PH, Giasson BI. The E46K mutation in alpha -synuclein increases amyloid fibril formation. J. Biol. Chem. 2005; 280:7800–7807. [PubMed: 15632170]

Hasegawa T, Matsuzaki M, Takeda A, Kikuchi A, Akita H, Perry G, Smith MA, Itoyama Y. Accelerated alpha-synuclein aggregation after differentiation of SH-SY5Y neuroblastoma cells. Brain Res. 2004; 1013:51–59. [PubMed: 15196967]

Hashimoto M, Hsu LJ, Sisk A, Xia Y, Takeda A, Sundsmo M, Masliah E. Human recombinant NACP/alpha-synuclein is aggregated and fibrillated in vitro: relevance for Lewy body disease. Brain Res. 1998; 799:301–306. [PubMed: 9675319]

Johnston JA, Ward CL, Kopito RR. Aggresomes: A Cellular Response to Misfolded Proteins. J. Cell Biol. 1998; 143:1883–1898. [PubMed: 9864362]

Kahle PJ, Neumann M, Ozmen L, et al. Hyperphosphorylation and insolubility of alpha-synuclein in transgenic mouse oligodendrocytes. EMBO Rep. 2002; 3:583–588. [PubMed: 12034752]

Klunk WE, Pettegrew JW, Abraham DJ. Quantitative evaluation of congo red binding to amyloid-like proteins with a beta-pleated sheet conformation. J. Histochem. Cytochem. 1989; 37:1273–1281. [PubMed: 2666510]

Koo HJ, Choi MY, Im H. Aggregation-defective alpha-synuclein mutants inhibit the fibrillation of Parkinson's disease-linked alpha-synuclein variants. Biochem. Biophys. Res. Commun. 2009; 386:165–169. [PubMed: 19501571]

Koo HJ, Lee HJ, Im H. Sequence determinants regulating fibrillation of human alpha-synuclein. Biochem. Biophys. Res. Commun. 2008; 368:772–778. [PubMed: 18261982]

Kordower JH, Chu Y, Hauser RA, Freeman TB, Olanow CW. Lewy body-like pathology in long-term embryonic nigral transplants in Parkinson's disease. Nat. Med. 2008; 14:504–506. [PubMed: 18391962]

Lee G, Tanaka M, Park K, Lee SS, Kim YM, Junn E, Lee SH, Mouradian MM. Casein kinase II-mediated phosphorylation regulates alpha-synuclein/synphilin-1 interaction and inclusion body formation. J. Biol. Chem. 2004; 279:6834–6839. [PubMed: 14645218]

Lee HJ, Shin SY, Choi C, Lee YH, Lee SJ. Formation and removal of alpha-synuclein aggregates in cells exposed to mitochondrial inhibitors. J. Biol. Chem. 2002; 277:5411–5417. [PubMed: 11724769]

Lee HJ, Suk JE, Bae EJ, Lee JH, Paik SR, Lee SJ. Assembly-dependent endocytosis and clearance of extracellular alpha-synuclein. Int. J Biochem. Cell Biol. 2008; 40:1835–1849. [PubMed: 18291704]

Lee HJ, Patel S, Lee SJ. Intravesicular localization and exocytosis of alpha-synuclein and its aggregates. J. Neurosci. 2005; 25:6016–6024. [PubMed: 15976091]

Lee VM, Trojanowski JQ. Mechanisms of Parkinson's disease linked to pathological alpha-synuclein: new targets for drug discovery. Neuron. 2006; 52:33–38. [PubMed: 17015225]

Li JY, Englund E, Holton JL, et al. Lewy bodies in grafted neurons in subjects with Parkinson's disease suggest host-to-graft disease propagation. Nat. Med. 2008; 14:501–503. [PubMed: 18391963]

Lippa CF, Schmidt ML, Lee VM, Trojanowski JQ. Dementia with Lewy bodies. Neurology. 1999; 52:893. [PubMed: 10078758]

Liu J, Zhang JP, Shi M, Quinn T, Bradner J, Beyer R, Chen S, Zhang J. Rab11a and HSP90 regulate recycling of extracellular alpha-synuclein. J. Neurosci. 2009; 29:1480–1485. [PubMed: 19193894]

Luk KC, Song C, O'Brien P, Stieber A, Branch JR, Brunden KR, Trojanowski JQ, Lee VM. Exogenous alpha-synuclein fibrils seed the formation of Lewy body-like intracellular inclusions in cultured cells. Proc. Natl. Acad. Sci U. S. A. 2009; 106:20051–20056. [PubMed: 19892735]

Mazzulli JR, Mishizen AJ, Giasson BI, Lynch DR, Thomas SA, Nakashima A, Nagatsu T, Ota A, Ischiropoulos H. Cytosolic catechols inhibit alpha-synuclein aggregation and facilitate the

formation of intracellular soluble oligomeric intermediates. J. Neurosci. 2006; 26:10068–10078. [PubMed: 17005870]

Murray IV, Giasson BI, Quinn SM, Koppaka V, Axelsen PH, Ischiropoulos H, Trojanowski JQ, Lee VM. Role of alpha-synuclein carboxy-terminus on fibril formation in vitro. Biochemistry. 2003; 42:8530–8540. [PubMed: 12859200]

Nedelsky NB, Todd PK, Taylor JP. Autophagy and the ubiquitin-proteasome system: Collaborators in neuroprotection. Biochimica et Biophysica Acta (BBA) - Molecular Basis of Disease. 2008; 1782:691–699.

Neumann M, Kahle PJ, Giasson BI, et al. Misfolded proteinase K-resistant hyperphosphorylated alpha-synuclein in aged transgenic mice with locomotor deterioration and in human alpha-synucleinopathies. J. Clin. Invest. 2002; 110:1429–1439. [PubMed: 12438441]

Nishie M, Mori F, Fujiwara H, Hasegawa M, Yoshimoto M, Iwatsubo T, Takahashi H, Wakabayashi K. Accumulation of phosphorylated alpha-synuclein in the brain and peripheral ganglia of patients with multiple system atrophy. Acta Neuropathol. (Berl). 2004; 107:292–298. [PubMed: 14722716]

O'Farrell C, Murphy DD, Petrucelli L, Singleton AB, Hussey J, Farrer M, Hardy J, Dickson DW, Cookson MR. Transfected synphilin-1 forms cytoplasmic inclusions in HEK293 cells. Mol. Brain. Res. 2001; 97:94–102. [PubMed: 11744167]

Opazo F, Krenz A, Heermann S, Schulz JB, Falkenburger BH. Accumulation and clearance of alpha-synuclein aggregates demonstrated by time-lapse imaging. J. Neurochem. 2008; 106:529–540. [PubMed: 18410502]

Pandey N, Schmidt RE, Galvin JE. The alpha-synuclein mutation E46K promotes aggregation in cultured cells. Exp. Neurol. 2006; 197:515–520. [PubMed: 16325180]

Paxinou E, Chen Q, Weisse M, Giasson BI, Norris EH, Rueter SM, Trojanowski JQ, Lee VMY, Ischiropoulos H. Induction of alpha-synuclein aggregation by intracellular nitrative insult. J. Neurosci. 2001; 21:8053–8061. [PubMed: 11588178]

Perrin RJ, Woods WS, Clayton DF, George JM. Interaction of human alpha-Synuclein and Parkinson's disease variants with phospholipids. Structural analysis using site-directed mutagenesis. J. Biol. Chem. 2000; 275:34393–34398. [PubMed: 10952980]

Polymeropoulos MH, Lavedan C, Leroy E, et al. Mutation in the alpha-synuclein gene identified in families with Parkinson's disease. Science. 1997; 276:2045–2047. [PubMed: 9197268]

Ren PH, Lauckner JE, Kachirskaia I, Heuser JE, Melki R, Kopito RR. Cytoplasmic penetration and persistent infection of mammalian cells by polyglutamine aggregates. Nat. Cell Biol. 2009; 11:219–225. [PubMed: 19151706]

Sampathu DM, Giasson BI, Pawlyk AC, Trojanowski JQ, Lee VM. Ubiquitination of alpha-synuclein is not required for formation of pathological inclusions in alpha-synucleinopathies. Am. J. Pathol. 2003; 163:91–100. [PubMed: 12819014]

Sidhu A, Wersinger C, Vernier P. Does alpha-synuclein modulate dopaminergic synaptic content and tone at the synapse? FASEB J. 2004; 18:637–647. [PubMed: 15054086]

Smith WW, Margolis RL, Li X, Troncoso JC, Lee MK, Dawson VL, Dawson TM, Iwatsubo T, Ross CA. Alpha-synuclein phosphorylation enhances eosinophilic cytoplasmic inclusion formation in SH-SY5Y cells. J. Neurosci. 2005; 25:5544–5552. [PubMed: 15944382]

Spillantini MG, Crowther RA, Jakes R, Cairns NJ, Lantos PL, Goedert M. Filamentous alpha-synuclein inclusions link multiple system atrophy with Parkinson's disease and dementia with Lewy bodies. Neurosci. Lett. 1998; 251:205–208. [PubMed: 9726379]

Spillantini MG, Schmidt ML, Lee VMY, Trojanowski JQ, Jakes R, Goedert M. Alpha-synuclein in Lewy bodies. Nature. 1997; 388:839–840. [PubMed: 9278044]

Tsuchiya K, Tajima H, Kuwae T, et al. Pro-apoptotic protein glyceraldehyde-3-phosphate dehydrogenase promotes the formation of Lewy body-like inclusions. Eur. J. Neurosci. 2005; 21:317–326. [PubMed: 15673432]

Tu PH, Galvin JE, Baba M, et al. Glial cytoplasmic inclusions in white matter oligodendrocytes of multiple system atrophy brains contain insoluble alpha-synuclein. Ann. Neurol. 1998; 44:415–422. [PubMed: 9749615]

Uversky VN, Cooper M, Bower KS, Li J, Fink AL. Accelerated alpha-synuclein fibrillation in crowded milieu. FEBS Lett. 2002; 515:99–103. [PubMed: 11943202]

von Bohlen Und HO. Synucleins and their relationship to Parkinson's disease. Cell Tissue Res. 2004; 318:163–174. [PubMed: 15503152]

Waelter S, Boeddrich A, Lurz R, Scherzinger E, Lueder G, Lehrach H, Wanker EE. Accumulation of Mutant Huntingtin Fragments in Aggresome-like Inclusion Bodies as a Result of Insufficient Protein Degradation. Mol. Biol. Cell. 2001; 12:1393–1407. [PubMed: 11359930]

Waxman EA, Covy JP, Bukh I, Li X, Dawson TM, Giasson BI. Leucine-rich repeat kinase 2 expression leads to aggresome formation that is not associated with alpha-synuclein inclusions. J Neuropathol. Exp. Neurol. 2009a; 68:785–796. [PubMed: 19535993]

Waxman EA, Duda JE, Giasson BI. Characterization of antibodies that selectively detect alpha-synuclein in pathological inclusions. Acta Neuropathol. 2008; 116:37–46. [PubMed: 18414880]

Waxman EA, Giasson BI. Specificity and regulation of casein kinase-mediated phosphorylation of alpha-synuclein. J. Neuropathol. Exp. Neurol. 2008; 67:402–416. [PubMed: 18451726]

Waxman EA, Mazzulli JR, Giasson BI. Characterization of hydrophobic residue requirements for alpha-synuclein fibrillization. Biochemistry. 2009b; 48:9427–9436. [PubMed: 19722699]

Wood SJ, Wypych J, Steavenson S, Louis JC, Citron M, Biere AL. alpha-synuclein fibrillogenesis is nucleation-dependent. Implications for the pathogenesis of Parkinson's disease. J. Biol. Chem. 1999; 274:19509–19512. [PubMed: 10391881]

Zhou W, Freed CR. Tyrosine-to-cysteine modification of human alpha-synuclein enhances protein aggregation and cellular toxicity. J. Biol. Chem. 2004; 279:10128–10135. [PubMed: 14699135]

Zhou Z, Fan JB, Zhu HL, et al. Crowded, cell-like environment accelerates the nucleation step of amyloidogenic protein misfolding. J. Biol. Chem. 2009; 284:30148–30158. [PubMed: 19748895]

Zhuang ZP, Kung MP, Hou C, Skovronsky DM, Gur TL, Plossl K, Trojanowski JQ, Lee VMY, Kung HF. Radioiodinated styrylbenzenes and thioflavins as probes for amyloid aggregates. J. Med. Chem. 2001; 44:1905–1914. [PubMed: 11384236]

Zibaee S, Jakes R, Fraser G, Serpell LC, Crowther RA, Goedert M. Sequence determinants for amyloid fibrillogenesis of human alpha-synuclein. J. Mol. Biol. 2007; 374:454–464. [PubMed: 17936783]

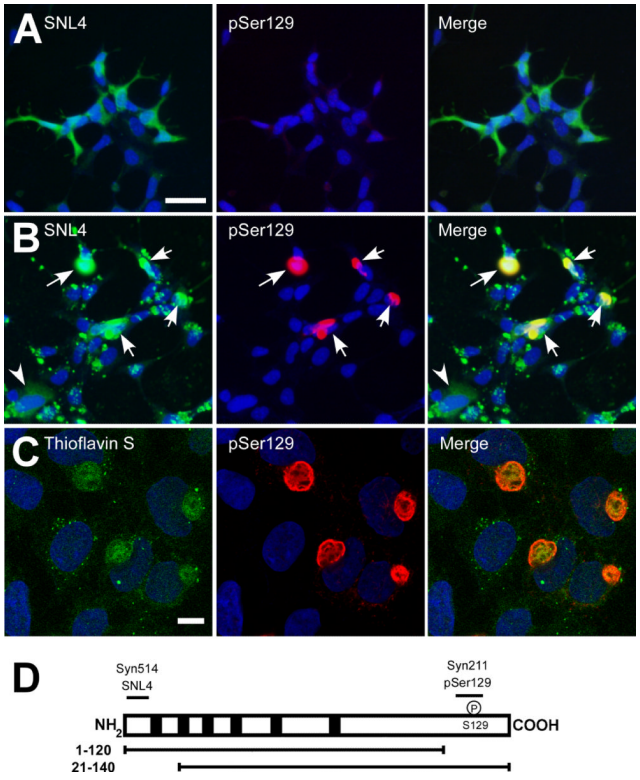

Figure 1.

Double-immunofluorescence with SNL4 **(green)** and pSer129 **(red)** on QBI293 cells transfected with WT α-syn in the absence **(A)** or presence **(B)** of recombinant, sonicated WT α-syn fibril treatment. α-Syn appeared diffuse in the absence of recombinant fibrils **(A)**. With recombinant fibril treatment **(B)**, a large number of large cellular aggregates were observed **(arrows)**. Faint immunostaining of transfected cells without cellular aggregates was also observed **(arrowhead)**. However, SNL4 also immunolabeled an overabundance of exogenous, recombinant fibrils. pSer129 immunolabeling more specifically recognized intracellular aggregates. **(C)** Confocal microscopy of double-immunofluorescence of QBI293 cells after transfection and treatment with recombinant fibrils. Immunostaining with thioflavin S **(green)** and pSer129 **(red)** showed abundant, large, fibrous intracellular aggregates that were thioflavin positive. Small punctae of thioflavin immunoreactivity was also observed, consistent with exogenous, recombinant fibrils. Bar scale = 50 μM for **A,B**; 10 μM for **C**. Representative confocal image is of a single Z-plane of <0.7 μm. **(D)** Schematic of human α-syn protein and epitopes of anti-α-syn antibodies. Diagram of α-syn shows the 6 imperfect “KTKEGV” repeats (black boxes). Epitopes of anti-α-syn specific antibodies are indicated in relationship to N-terminal (21–140) and C-terminal (1–120) truncated α-syn. Antibodies Syn514 and SNL4 recognize the N-terminus and require amino acids 2–12. Syn211 recognizes amino acids 125–129. pSer129 was raised against a phospho-peptide from amino acids 123–134 and specifically recognizes phosphorylation at residue Ser129.

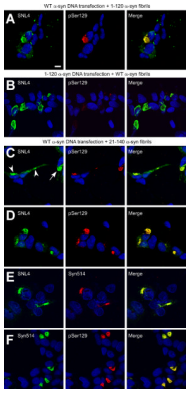

Figure 2.

Confocal microscopy of double-immunofluorescence of QBI293 cells after transfection and seeding with recombinant α-syn fibrils. Cells were transfected with WT α-syn **(A,C,D,E,F)** or 1–120 α-syn **(B)** expression plasmids, and then treated with 1 μM of recombinant *in vitro* generated WT α-syn **(B)**, 1–120 α-syn **(A)**, or 21–140 α-syn **(C–F)** that had been fibrillized and sonicated prior to addition to the medium (fibrils). Double-immunofluorescence was performed between α-syn-specific antibodies SNL4 and pSer129 **(A–D)**, SNL4 and Syn514 **(E)**, or Syn514 and pSer129 **(F)**. The extracellular addition of fibrils induced the formation of large, fibrous aggregates. Representative images were of cells fixed 48 hr after removal of calcium phosphate. Panel C shows cells containing small aggregates **(arrowheads)** that are early in formation, where the majority of intracellular α-syn appears soluble and diffuse. Epitope-specificity of antibodies used indicates that the intracellular α-syn aggregates are primarily composed of endogenously expressed α-syn. Representative images are of a single Z-plane of <0.7 μm. Bar scale = 10 μm.

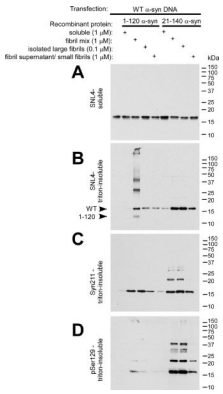

Figure 3.

Biochemical cellular fractionation of QBI293 cells after transfection and seeding with recombinant α-syn fibrils. QBI293 cells were transfected with the WT α-syn expression plasmid. After transfection, recombinant 1–120 α-syn or 21–140 α-syn was added to the media. The recombinant protein was added in soluble form, after fibrillization *in vitro* (fibril mix), or after fibrillization and isolation by centrifugation at 16,000 × *g*, where the pellet (large fibrils) was isolated from the supernatant (small fibrils/polymers/soluble protein). Western blot analysis of α-syn immunoreactivity was performed after biochemical cellular fractionation isolating soluble from triton-insoluble α-syn, as described in "Materials and Methods." The first lane at the left shows biochemical fractionation of cells that did not receive any recombinant α-syn treatment. **(A)** SNL4 immunoreactivity of soluble samples recognized soluble WT α-syn, resulting from cellular transfection. Triton-insoluble protein was analyzed with **(B)** SNL4, **(C)** Syn211, and **(D)** pSer129 antibodies, and α-syn was identified in samples treated with recombinant fibrillized α-syn protein. Migration of α-syn protein and epitope-specific antibodies show that the addition of recombinant fibrillized protein induced aggregation of endogenously expressed α-syn. Arrowheads indicate the immunobands corresponding to full-length WT α-syn (WT) and 1–120 α-syn (1–120).

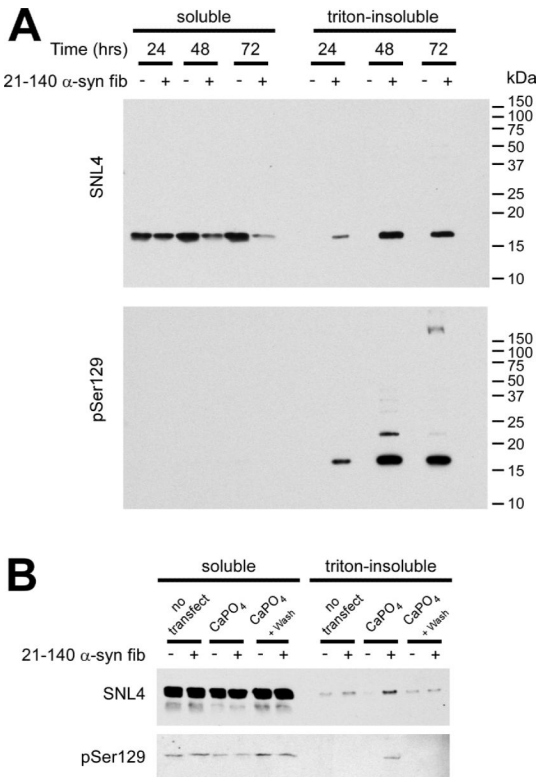

Figure 4.

Biochemical fractionation of QBI293 cells and SH-SY5Y neuroblastoma after recombinant α-syn fibril mix treatment. **(A)** Representative immunoblot of biochemical cellular fractionation of QBI293 cells over the course of time. Cells were transfected with the WT α-syn expression plasmid and examined with or without recombinant 21–140 α-syn fibril mix treatment (fib). Western blot analyses show an increase in triton-insoluble, phosphorylated α-syn from 24 hours (after calcium phosphate precipitation removal), to 48 hours and was maintained at 72 hours. **(B)** SH-SY5Y neuroblastoma that were stably transfected with WT α-syn were treated with 1 μM of recombinant 21–140 α-syn fibril mix (fib) either with or without calcium phosphate precipitation ($CaPO_4$) using a control DNA plasmid (pcDNA3.1). Cells were harvested at 48 hours (after calcium phosphate precipitation removal). Representative immunoblot indicated an increase in triton-insoluble, phosphorylated α-syn only with treatment of both $CaPO_4$ and 21–140 α-syn fibril mix.

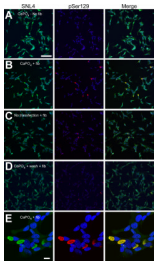

Figure 5.

Double-immunofluorescence of SH-SY5Y neuroblastoma after recombinant α-syn fibril mix treatment. Double-immunofluorescence was performed with SNL4 **(green)** and pSer129 **(red)** on SH-SY5Y neuroblastoma that were stably transfected with WT α-syn. Cells were treated with calcium phosphate precipitation ($CaPO_4$) using the control pcDNA3.1 plasmid **(A,B,D,E)** and/or recombinant 21–140 α-syn fibril mix (fib) **(B–E)**. Removal of $CaPO_4$ (wash), followed by fibril mix treatment was also investigated **(D)**. α-Syn aggregates were formed when cells were treated with recombinant α-syn fibril mix; however, a significant increase in the propensity to form aggregates was observed with concomitant treatment of both $CaPO_4$ and fibrils. **(E)** Confocal microscopy image of α-syn aggregates in SH-SY5Y neuroblastoma. Bar scale = 100 μm for A–D; 10 μm for E.

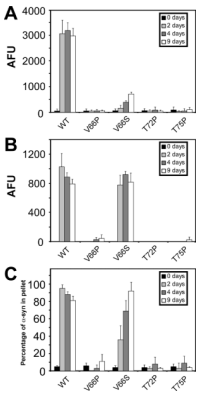

Figure 6.

α-Syn proteins with mutations in the hydrophobic region inhibit *in vitro* fibrillization. **(A)** ThT fluorometry, **(B)** K114 fluorometry, and **(C)** quantitative sedimentation analysis of the formation of large polymers and amyloid for WT, V66P, V66S, T72P, or T75P α-syn after 0, 2, 4 and 9 days of incubation under assembly conditions, as described in "Materials and Methods." All proteins were incubated at 5 mg/ml. Data represent average ± SD. n = 6 for ThT and K114 fluorometry, and n = 3 for sedimentation analysis.

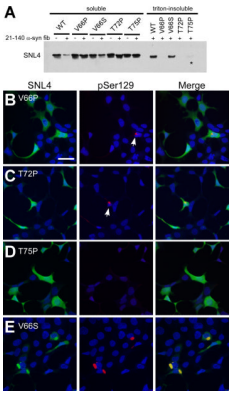

Figure 7.

Comparative biochemical fractionation and double-immunofluorescence analyses of QBI293 cells expressing WT α-syn or α-syn containing single-point mutations. **(A)** Representative immunoblot of biochemical fractionation on cells transfected with plasmids expressing WT, V66P, V66S, T72P, or T75P human α-syn. Treatment with recombinant 21–140 α-syn fibril mix (fib) produced triton-insoluble WT and V66S α-syn protein. Triton-insoluble T75P α-syn was observed in the experiment shown, but was present at low levels, and only present in one set of experiments (n=5, asterisk (*)). Triton-insoluble α-syn was not observed in the absence of fibril mix treatment (data not shown). **(B–E)** Double-immunofluorescence on QBI293 cells that were transfected with plasmids for the expression of **(B)** V66P α-syn, **(C)** T72P α-syn, **(D)** T75P α-syn, or **(E)** V66S α-syn. All conditions were treated with recombinant 21–140 α-syn fibril mix. Double-immunofluorescence between SNL4 **(green)** and pSer129 **(red)** antibodies shows that cells expressing V66P or T72P α-syn developed small, infrequent pSer129-positive aggregates **(arrows)**. Cells expressing T75P α-syn and treated with recombinant α-syn fibril mix did not present any pSer129-positive aggregates. Microscopic analysis of cells expressing V66S α-syn **(E)** was indistinguishable from cells expressing WT α-syn. Bar scale = 50 μm.

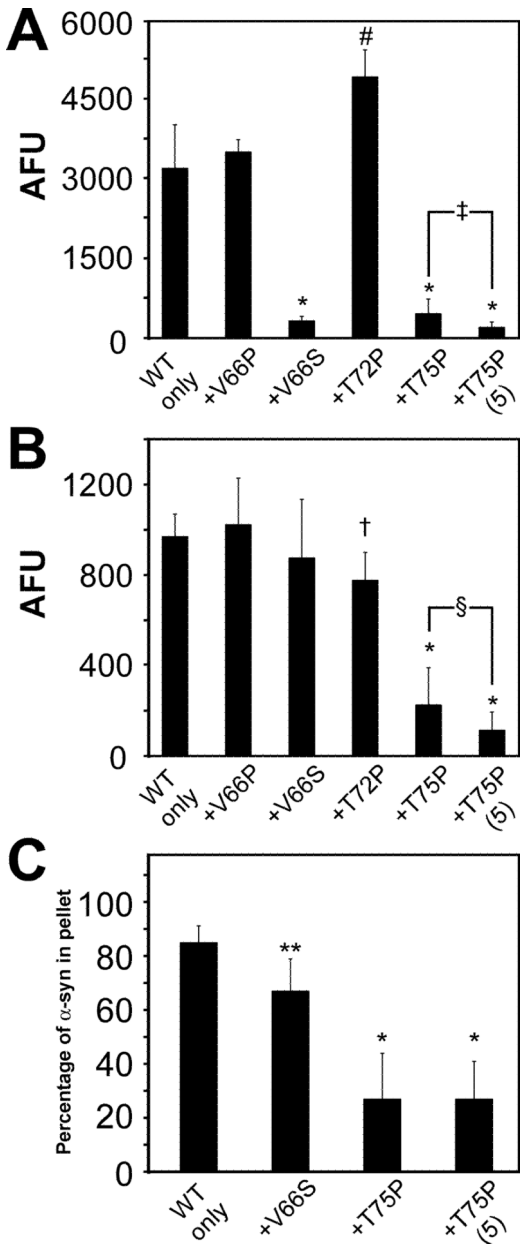

Figure 8.

Effects of α-syn proteins with mutations in the hydrophobic region on the polymerization of WT α-syn *in vitro*. **(A)** ThT fluorometry, **(B)** K114 fluorometry, and **(C)** quantitative sedimentation analysis of the formation of amyloid and large polymers for recombinant WT α-syn alone or co-incubated with (+) recombinant α-syn that has been mutated at V66P, V66S, T72P, or T75P. All proteins were incubated at 2.5 mg/ml (for a total of 5 mg/ml in conditions containing both WT and mutant protein) for 4 days. Condition indicated as "+T75P (5)" is that of WT α-syn at 2.5 mg/ml incubated with T75P α-syn at 5 mg/ml. Data represent average ± SD. *, $p < 0.0001$; #, $p = 0.0003$; ‡, $p = 0.003$; †, $p = 0.002$; §, $p = 0.03$; **, $p = 0.01$. n=6 for V66P α-syn and T72P α-syn; n=8 for V66S α-syn; n=14 for T75P α-syn K114 and ThT fluorometry; and n=4 for all sedimentation analyses.

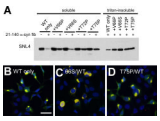

Figure 9.

Biochemical fractionation and double-immunofluorescence analysis of QBI293 cells co-expressing WT and mutant α-syn and treated with recombinant α-syn fibril mix. **(A)** Representative immunoblot with antibody SNL4 of biochemically fractionated cells co-transfected with the WT α-syn expression plasmid with empty pcDNA3.1 vector (WT only), or with two plasmids for expression of both WT and V66P α-syn (+V66P), WT and V66S α-syn (+V66S), WT and T72P α-syn (+T72P), or WT and T75P α-syn (+T75P). Treatment with recombinant 21–140 α-syn fibril mix (fib) produced triton-insoluble α-syn in all conditions. Triton-insoluble α-syn was not observed in the absence of fib treatment (data not shown). n = 4. **(B–D)** Double-immunofluorescence with SNL4 **(green)** and pSer129 **(red)** on QBI293 cells that were transfected with two plasmids for expression of **(B)** WT α-syn and pcDNA3.1 (WT only), **(C)** WT α-syn and V66S α-syn, or **(D)** WT α-syn and T75P α-syn. All conditions formed frequent SNL4 and pSer129 positive aggregates **(yellow)** that were indistinguishable from cells transfected with only the WT α-syn plasmid. Only merged images are shown. Bar scale = 50 μm.